NEUTRAL HYDROGEN IN THE UNIVERSE

F. H. BRIGGS
Australian National University, Mount Stromlo Observatory,
Cotter Road, Weston Creek, ACT 2611, Australia
and
Australia National Telescope Facility
PO Box 76, Epping, NSW 1710, Australia
E-mail: fbriggs@mso.anu.edu.au

Neutral atomic hydrogen is an endangered species at the present age of the Universe. When hydrogen is dispersed at low density in the intergalactic medium, the gas is vulnerable to photoionization, and once ionized, the time time for recombination exceeds the Hubble time. If hydrogen clouds are confined to sufficient density that they are self-shielding to the ionizing background, they are vulnerable to instability, collapse and star formation, which over time, locks the hydrogen into long lived stars. When neutral clouds do exist after the Epoch of Reionization, they associate closely with galaxies; in these locations, they provide valuable kinematical tracers of the gravitational potentials that bind galaxies and groups.

1 Introduction

Although hydrogen is always portrayed as "the most abundant" of the elements in the Universe, atoms of hydrogen are actually rare. Most of the hydrogen spends most of its time in an ionized state – namely, in an plasma of protons and electrons, accompanied by the ionized nuclei of helium and traces of heavier elements. Here and there, clouds of neutral, atomic hydrogen do exist, but these clouds find themselves confined to large gravitational potential wells, which they share with stars; the clouds rely on the gravity that holds galaxies together to also confine the hydrogen to relatively high density, which makes the clouds less vulnerable to photoionization. But in this environment, they become more vulnerable to instability, collapse and star formation, and for that reason there is a close association of neutral-gas-richness with star formation.

Astronomers study the kinematics of the hydrogen clouds in galaxies, since their motion is a tracer of the depth and shape of the gravitational potential. Observations to inventory of the neutral gas content of galaxies measure of the reservoir of fuel that is readily available for forming new stars.

Figure 1 gives an overview of the history of neutral gas clouds over the age of the Universe. It begins at the phase transition corresponding to the release of the Cosmic Microwave Background photons (at $z \sim 1100$), when the ionized baryons and elections combine to become a neutral gas, commonly labeled HI by astronomers, and which is composed of H^o atoms (in chemical notation). Along with the hydrogen, the primordial mix includes some helium and a trace of lithium. There follows the only period, lasting about 100 million years, when the majority of the Universe's atoms are neutral. This period, known as the 'Dark Age,' ends when the first objects collapse as a result of gravitational instability, providing sources of ionizing energy. We refer to the end of the Dark Age as the 'Epoch of Reionization' (EoR), when the H^o atoms become H^+ (and the HI becomes HII). We associate

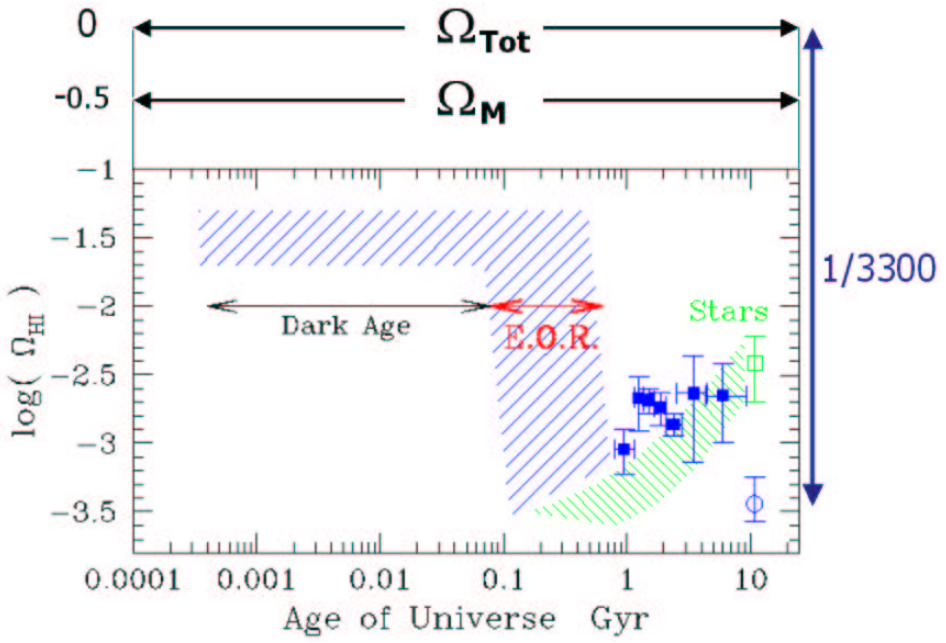

Figure 1. History of the neutral hydrogen content of the Universe. The logarithm of the neutral gas density normalized to the 'closure density' necessary to close the Universe is plotted as a function of the age of the Universe. Square filled points are measurements from Damped Lyman-α QSO absorption-line statistics. The open circle at far right represents the neutral gas content of the present day ($z = 0$) Universe. For comparison, the rising trend of stellar mass content appears has a hatched envelope, which increases to the value measured at $z = 0$ from the optical luminosity density of stars.

the EoR with the onset of the first generation of stars (which form in the most overdense regions) and the appearance of protogalactic objects, which become the building blocks of structure – leading to galaxies and clusters of galaxies, as the forces of gravity run their course.

In the diagram of Fig. 1, the EoR is also marked by the appearance of a second shaded region that indicates schematically the beginnings of the build up of mass in stars, as subsequent generations of star formation gradually lock increasing numbers of baryons into low mass, long lived stars. The stellar mass content of the Universe rises steadily from the EoR to the present, where we have precise measurements through meticulous inventories of the numbers of galaxies and their luminosities (i.e., the galaxy luminosity function and the integral luminosity density)(see for instance, Madgwick et al 2002).

Astronomers can also make accurate measures of the neutral gas content at the present epoch (for instance, Zwaan et al 2003). These result from the direct detection of the radio spectral line emission from atomic hydrogen at 21cm wavelength, and the observations lead to an HI Mass Function for neutral gas clouds (which is analogous to the optical luminosity function for galaxies) to quantify the relative

numbers of small and large clouds.

Through the period following the EoR, astronomers have statistical measures of the HI content as a function of time through the observation of QSO absorption lines. Any gas rich object that populates the Universe has a random chance of intervening along the line sight to distant objects. Quasi-stellar objects are especially useful as background sources since they have strong optical and UV continuum emission against which intervening gas clouds can imprint a distinctive absorption line spectrum. In the case of thick clouds of neutral gas, the Lyman-α line of HI is so strong that it presents an easily recognized 'damping wing' profile, which has led to the Damped Lyman-α (DLA) class of QSO absorption line (Wolfe et al 1986); in the minds of most astronomers, the DLAs are associated with gas-rich protogalaxies, which are the precursors of the larger galaxies that we observe around us at present (Prochaska & Wolfe 1997, Haenelt et al 1998).

The measure of Ω_{HI} during the Dark Age is substantiated by the remarkable agreement of two very difference techniques: (1) the measurement of the abundances of the light elements (deuterium, helium, and Lithium) and the constraints they impose on primordial nucleosynthesis (Olive et al 2000), and (2) the measurement of the fluctuation spectrum of the CMB, which specifies a number of cosmological parameters, including the baryon number density (Spergel et al 2003). For purposes of constructing Fig. 1, all of the Universal baryons are assumed to be locked into their neutral atomic form throughout the Dark Age.

A further consequence of the precise cosmological measurements that have resulted from studies of the CMB is that we can compare the relative importance of atomic hydrogen throughout history with the dominant constituents: the dark matter and the dark energy (Spergel et al 2003). As indicated in Fig.1, the current best cosmological model has a flat Universe ($\Omega_{tot} = 1$), with the mass density contributing $\Omega_M \approx 0.3$ and a dark energy providing $\Omega_\Lambda \approx 0.7$. The mass density is dominated by the dark matter component, which accounts for 84 percent of Ω_M. Especially at present, the Ω_{HI} amounts to a tiny fraction of the mass-energy budget of the Universe.

The following sections elaborate the conditions that hydrogen gas experiences, focusing on why there are so few HI clouds remain once the EoR has occurred, the use of HI as a kinematic tracer, and the expectation that radio observations of the 21cm line will help to elucidate the processes that ended the Dark Age.

2 Observing Hydrogen

Astronomers can observe hydrogen because it emits and absorbs light. The internal structure of the atom allows only discrete energy levels, and this limits the photon energies that can be exchanged with the atom, and it also makes clear under what conditions various spectral lines would be expected to occur. Figure 2 sketches the energy levels for atomic hydrogen.

Hydrogen clouds have long been observed in our galaxy in HII regions and planetary nebulae, where the Balmer series lines are seen in emission. The energy levels that produce the Balmer lines must be populated, in order for them to radiatively decay (by emitting a photon) to reach the $n = 2$ first excited state. In Galactic neb-

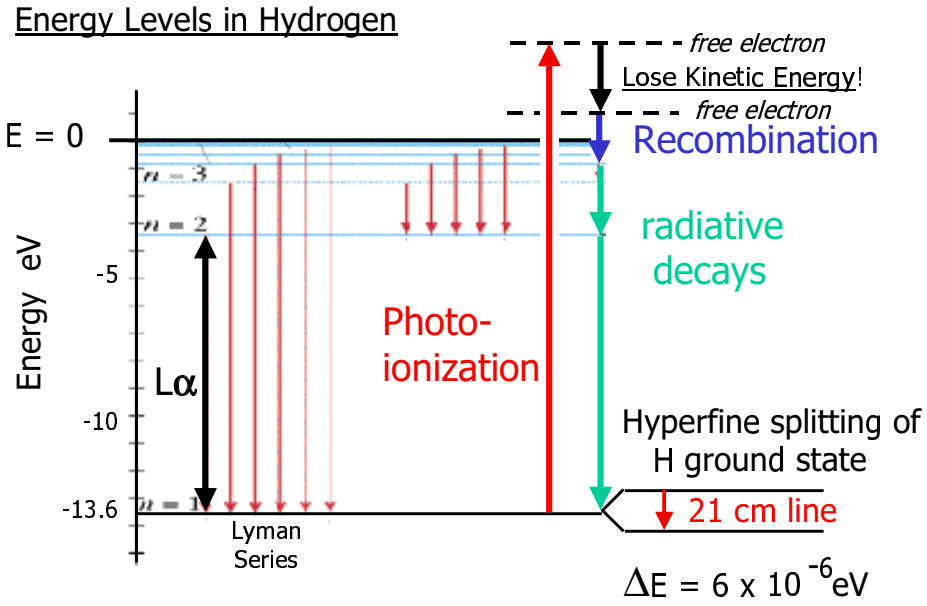

Figure 2. The Energy Level diagram for the Hydrogen atom, with annotations for (1) The Lyman series, with Lyman-α (Lα) marked, (2) the photoionization-recombination cycle indicated, with photoionization from the ground state followed by the free electron heating the surrounding plasma by losing kinetic energy to collisions, and the radiative recombination leading to emission of photons through radiative decay, and (3) the small hyperfine splitting of the ground state to give rise to the 21cm line.

ulae, this is accomplished by photoionizing the nebulae with ionizing, UV photons from hot stars, followed by recombination and radiative decay. Also important in this process is the energy lost by the photoelectron, as it is scattered in the nebula, since this is the source of heating for the gas. Clearly, they are the ionized hydrogen clouds – not the neutral ones – that radiated effectively.

Neutral hydrogen in galaxies is cool with temperatures ranging from ~50 to a few hundred degrees for the clouds to a few thousand degrees for the warm phase, intercloud medium (Wolfire et al 2003, Liszt 2001). These temperatures are too low to excite the atoms to the $n = 2$ level or above, so there are seldom excited atoms capable of emitting or absorbing Balmer wavelength photons. (This situation is clearly very different from the hydrogen in the atmospheres of stars where temperatures and densities are high enough to excite the $n = 2$ level, allowing the Balmer lines to have a long history in helping to classify stars through absorption line spectroscopy at optical wavelengths.) Cool hydrogen cannot absorb optical wavelengths, but it is very effective at absorbing in the ultra-violet Lyman lines and in the"Lyman continuum," which is the wavelength range corresponding to ionizing photons with energies greater than 13.6 eV.

Fortunately, atomic hydrogen has another low lying energy level that arises from a tiny, "hyperfine" splitting of the $n = 1$ ground state. This allows hydrogen to emit and absorb photons with the radio wavelength 21.1 cm. A qualitative

interpretation of this splitting is that it arises from the relative alignment of the magnetic moments of spinning charges of the electron and proton; the quantum mechanics of the hydrogen atom allows for only two possible alignments, and there are therefore only two energy levels in the split ground state. The energy required to change the alignment is so small that weak collisions can excite and de-excite the hyperfine levels. This means that the kinetic temperature of the gas cloud, T_K, is effective at setting the hydrogen spin temperature, T_S, which governs the hyperfine level populations according to

$$\frac{N_+}{N_-} = \frac{g_+}{g_-} \exp\left(-\frac{\Delta E}{kT_S}\right) \approx \frac{g_+}{g_-} \exp\left(-\frac{h\nu}{kT_K}\right) \quad (1)$$

where g_+ and g_- are the degeneracies of the upper and lower levels ($g_+/g_- = 3$), $\Delta E \sim 6 \times 10^{-6}$eV (the energy of a $\lambda = 21$cm photon), and k is the Boltzmann constant. Under dilute conditions where atomic collisions become infrequent, then collisions with photons may dominate in setting the N_+/N_- ratio. For example, at the end of the Dark Age, the intergalactic medium has become sufficiently diffuse that the CMB photons will pin $T_S \approx T_{CMB} = 2.73(1+z)$K; once substantial overdensities evolve, the gas again becomes coupled to the gas kinetic temperature.

In summary, neutral hydrogen clouds are always capable of emitting 21cm line photons. If they chance to fall between the observer and a bright radio continuum source, then 21cm line absorption lines may be seen. Neutral hydrogen clouds do not absorb optical or infrared wavelength hydrogen lines (the Balmer or Paschen series for example), but they are strong absorbers of the ultraviolet Lyman lines, and they are effective at absorbing photons with energies greater than 13.6 eV (wavelengths $\lambda < 911$Å). All neutral clouds observed so far have traces of "metals" – elemental species heavier than helium, such as NaI and CaII – that may allow the clouds be detected in optical wavelength absorption lines when they are observed against sufficiently bright background stars or QSOs; neutral clouds also show very strong absorption in UV absorption lines by species such as MgI, MgII, FeII, SiII, CII, OI, AlII, among others. Neutral clouds do not emit optical or UV photons, unless they a bathed in a radiation field of energetic, ionizing photons, in which case they may become detectable in the recombination lines.

3 Hydrogen in the nearby Universe

Even now, some 13.7 billion years after the Big Bang according to the WMAP "concordance cosmology" (Spergel et al 2003), hydrogen remains the most abundant element. Estimates for where the baryons are located in the present day Universe are plotted in Fig. 1, where the stellar mass and neutral gas components account for $\Omega_*(z=0) \sim 0.004$ and $\Omega_{HI}(z=0) \sim 0.0004$. The WMAP cosmology has a baryonic mass density of $\Omega_{baryon} = 0.0044$ with total matter $\Omega_m = 0.27$.

Roughly 90% of the Univeral baryons in Fig. 1 remain unaccounted for at the present epoch in Fig. 1, since the sum of the mass in stars and the neutral gas clouds at $z = 0$ is far less than those produced in the Big Bang. A more complete census (Shull 2003, Penton et al 2000) finds that many of the missing baryons fill the vaste ionized sea that comprises the intergalactic medium (IGM). At present, the IGM

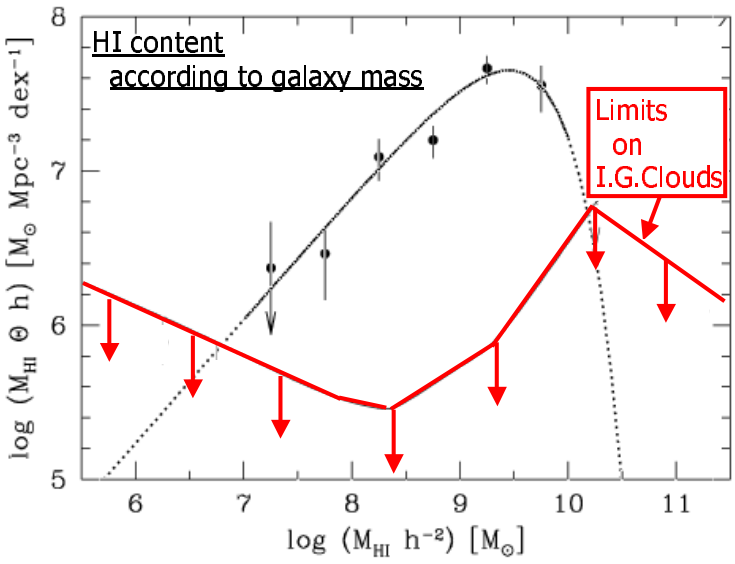

Figure 3. The integral neutral gas content of galaxies as a function of HI mass, showing that the more massive systems around $M^*_{HI} \sim 10^{9.55} h^{-2} \mathrm{M}_\odot$ (for $h = H_o/100$ km s^{-1}) are the dominant repositories of neutral gas at $z \approx 0$. Current limits on the abundances of intergalactic HI clouds permit no competitive amounts of neutral gas anywhere in the mass range characteristic of galactic systems (Zwaan et al 1997).

is of such low density that, once ionized, the recombination time greatly exceeds a Hubble time (see discussion in Section 5.1). Their presence is observable through the small fraction $n^0/(n^+ + n^0) \sim 10^{-3}$ of neutrals in the Lyman-α forest clouds (see Peterson, these proceedings) and through the traces of highly ionized species (CIV and OVI) indicating low level metal pollution of the IGM due to stellar mass loss over the age of the Universe (Shull 2003).

Here and there within the sea of ions and electrons, there are "condensations" where higher densities of baryons have undergone gravitational collapse that led to star formation. Each of the condensations formed within the confining potential well of a dark matter halo. A consistent picture of structure formation has the baryonic material being carried along into the evolving halos in constant proportion to the dark matter. Once confined in the halo, the baryons cool and gravo-thermal instabilities cause the gas clouds to collapse and form stars, leading to the objects we call galaxies.

The neutral baryons are but a small fraction of the total mass. Their distribution among galaxies of different types and sizes has been carefully measured (for example, Roberts & Haynes 1994). The general rule is that the late-type spiral and irregular galaxies are the richest in HI, consistent with their blue colors and populations of young stars. The elliptical and S0 galaxies are generally devoid of HI, in accord with their older stellar populations, although they occasionally have outlying HI clouds of substantial mass (Oosterloo et al 2003).

The HI mass function (HIMF) quantifies the relative number of galaxies with different HI masses in the same way that the optical luminosity function gives the numbers of galaxies of different luminosities. The main features of both the HIMF and the luminosity function are described by an analytic form called a Schechter Function (Schechter 1976). The HIMF has a functional dependence $\Theta(M_{HI})$ on HI mass M_{HI}:

$$\Theta(M_{HI})dM_{HI} = \Theta^* \left(\frac{M_{HI}}{M^*_{HI}}\right)^{-\alpha} \exp\left(-\frac{M_{HI}}{M^*_{HI}}\right) dM_{HI} \qquad (2)$$

with three parameters Θ^*, α, and M^*_{HI} that fix the shape and normalization. Plots of these functions on log-log axes make clear that the M^*_{HI} is the break point or "knee" that sets the high mass cutoff to the distribution; an exponential becomes a fairly hard cutoff on a log-log plot. The distribution below the cutoff is set by the power law slope α, and Θ^* specifies the normalization of the curve. The HIPASS survey with the Parkes Telescope has provided recent determinations of the parameters: $\Theta^* = (8.6 \pm 2.1)\times 10^{-3} h_{75}^{-3}\mathrm{Mpc}^{-3}$, $\alpha = 1.30 \pm 0.08$, and $M^*_{HI} = (6.1 \pm 0.9)\times 10^9 h_{75}^{-2}$

While the HIMF specifies the number of galaxies per Mpc^3 as a function of mass, a more useful plot for assessing the relative importance of the different mass ranges in the HI census is a plot of $\psi(M_{HI}) = \Theta(M_{HI})dM_{HI}/d\log_{10}M_{HI} = M_{HI} \ln 10\ \Theta(M_{HI})$, which compares the total amount of HI mass per Mpc^3, showing the galaxy population has in each logarithmic interval of M_{HI}. Fig. 3 has an example, where the HI density $\mathrm{M}_\odot\mathrm{Mpc}^{-3}$ is calculated per decade of HI mass. The peak near $10^{9.4} h_{100}^{-2}\mathrm{M}_\odot$ indicates that these galaxies with HI masses near the knee are the most important contributors of HI mass. Although the HIMF has a greater number of small masses per Mpc^3, the rarer large galaxies add up to a larger integral mass density. The sharp exponential cutoff to the HIMF indicates a very low contribution from galaxies with $M_{HI} > 10^{10.5}\mathrm{M}_\odot$.

A number of radio surveys in the 21cm line have blindly scanned the sky in search of intergalactic hydrogen clouds. To qualify as an "intergalactic cloud," a cloud must be isolated from any galactic system that emits starlight. The goal has been to find HI clouds that are confined to their own dark matter potential well without an accompanying stellar population. The surveys are considered "blind" when the region for the study has been chosen without regard for any prior knowledge of the numbers or types of optically identified galaxies in the region.

More than 20 years ago, Fisher and Tully (1981) deduced that the amount of mass in HI clouds was not cosmologically significant. That is to say, the integral mass content of a possible intergalactic cloud population did not come close to being enough to close the Universe by bringing its mass density up to the critical density. They arrived at this deduction by noting that every 21cm line observation made to catalog the HI mass in a nearby galaxy also includes a comparable amount of integration on blank sky nearby the galaxy. These blank sky observations are taken to calibrate the instrumental spectral passband shape on a galaxy by galaxy basis. Fisher and Tully found no HI signals in the off-source scans that were not associated with galaxies in the off-galaxy calibration spectra. Ten years later, Briggs (1990) made a similar analysis of the large number of new observations that had

been obtained using the same observing technique, and he concluded that in the HI mass range of $\sim 10^8$ to $10^{10} M_\odot$ that intergalactic HI clouds must be rare; they had to be outnumbered by galaxies with HI masses in this range by at least 100:1.

Since 1990, radio spectrographs have become better suited for making truly blind surveys of large areas of sky, resulting in a number of studies: Zwaan et al (1997), Spitzak & Schneider (1998), Kraan-Korteweg et al (1999), Rosenberg & Schneider (2000), Koribalski, B.S. et al (2003). Despite detecting thousands of galaxies in the hydrogen line, these survey have turned up no "free-floating" HI clouds (i.e., clouds that are not associated with the gravitational potential containing a population of stars).

Blitz et al (1999) and Braun and Burton (1999) have explored the possibility that the infalling population of small HI clouds associated with the halo of the Milky Way Galaxy – the "High Velocity Clouds" – are remnants of a primordial extragalactic population. In this scenario, the HI masses of the clouds would typically be larger than $\sim 10^7 M_\odot$, and every large galaxy should be surrounded by a similar halo of a few hundred of these objects if the phenomenon is a genuine and common feature of galaxy formation and evolution. The fact that nearby galaxies and groups do not possess such a halo of small clouds (Zwaan & Briggs 2000, Zwaan 2001) has ruled out this idea, requiring that the clouds must be an order of magnitude less massive and fall at distances within ~200 kpc of the Milky Way, well within our Galaxy's halo.

The clear association of neutral gas clouds with star-bearing galaxies implies that the HI relies on the confinement of the galaxies' gravitational potentials for their survival (see Sect. 5.1).

4 Redshifted HI in evolving galaxies

Radio astronomers would like to extend these kinds of 21cm emission line studies to higher redshifts, in order to monitor the amount of HI as a function of time and its relation to star forming regions. Unfortunately, the inverse-square law very quickly takes its toll, and the current generation of radio telescope cannot detect individual galaxies at redshifts much beyond 0.2. For this reason, much of what we know about the neutral gas content as a function of age of the Universe comes from the statistical analysis of the QSO absorption-lines. The next generation of radio telescopes has the design goal of being able to detect individual galaxies in the 21cm line to redshifts around three.

4.1 QSO absorption lines

Much of what we know about the gas content – both neutral and ionized – in evolving galactic systems over the redshift range from 6 to close to the present comes from the study of QSO absorption-lines. The strong ultra-violet continua of active galactic nuclei make fine sources of fairly clean background spectrum against which the intervening gas clouds imprint their distinctive absorption signatures. The QSOs themselves are marked by characteristic, broad emission lines that indicate the emission redshift; occasional "associated" narrow-line absorption occurs in the

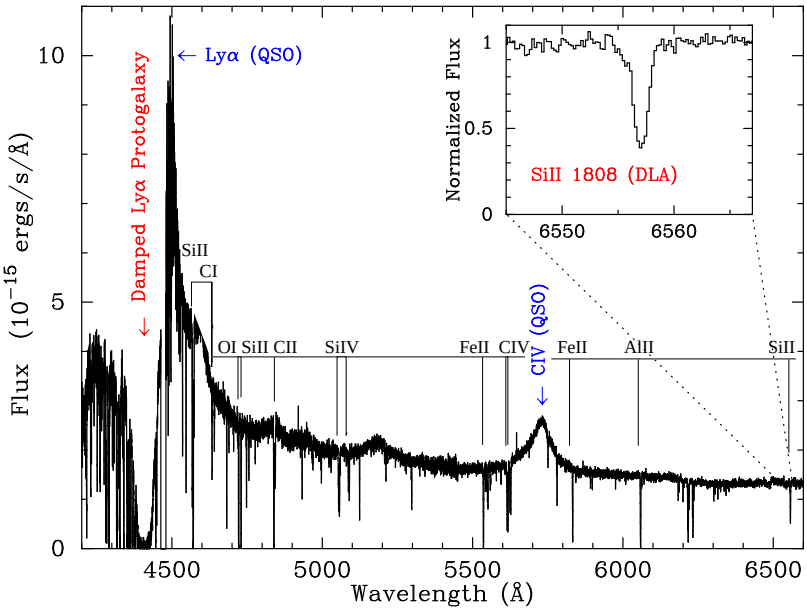

Figure 4. Spectrum of the $z_{em} = 2.701$ QSO FJ081240.6+320808, showing broad emission lines of the QSO (Ly-α and CIV are labeled) and absorption lines in a DLA system at $z = 2.626$, including the damped Lyman-α line and narrow metal lines. The inset box shows a zoom in on one of the weaker lines (SiII 1808) in this system. (figure courtesy of Prochaska et al 2003).

QSO host galaxy, and outflowing material from the nucleus causes broad absorption lines (BALs) in some 5-10% of QSOs.

The class of QSO absorption-line that occurs when intervening protogalaxies chance to fall along the sightline to a higher redshift QSO has much to tell us about the amounts of neutral and ionized gas as a function of time, the metal abundances, and kinematics in the intervenor.

The statistics for QSO absorption lines are typically analyzed by keeping track of the rate of intervention per unit redshift for each of the species (like triply ionized carbon, CIV, or singly ionized magnesium MgII) separately. This interception rate as a function of redshift is named $n(z) = dN/dz$ and called D-N-D-Z. Clearly it is inversely proportional to the mean-free-path between absorptions. The mean-free-path is related to the number density and cross-section of the absorbers $l_o = 1/n_o\sigma_o$. For a distribution of galaxy sizes, the expression generalizes to an integral, where n_o becomes the luminosity function $\Phi(L)$, and σ_o adopts a dependence on galaxy properties, including luminosity $\sigma(L)$. The fiducial luminosity L^* is the common reference for comparison, so QSO absorption-line discussions often quote cross-sections as though they were computed for L^* galaxies with non-evolving co-moving density. Fig. 5 illustrates this idea by presenting the cross-sections that non-evolving L^* galaxies would need to have to explain the intervention statistics for the species HI, CIV and MgII in the redshift range approximately 1 to 2.5. In fact, the rest wavelengths of these ions are substantially different so that the extensive ground-based observations monitor the $dN/dz(z)$ dependence over different redshift ranges

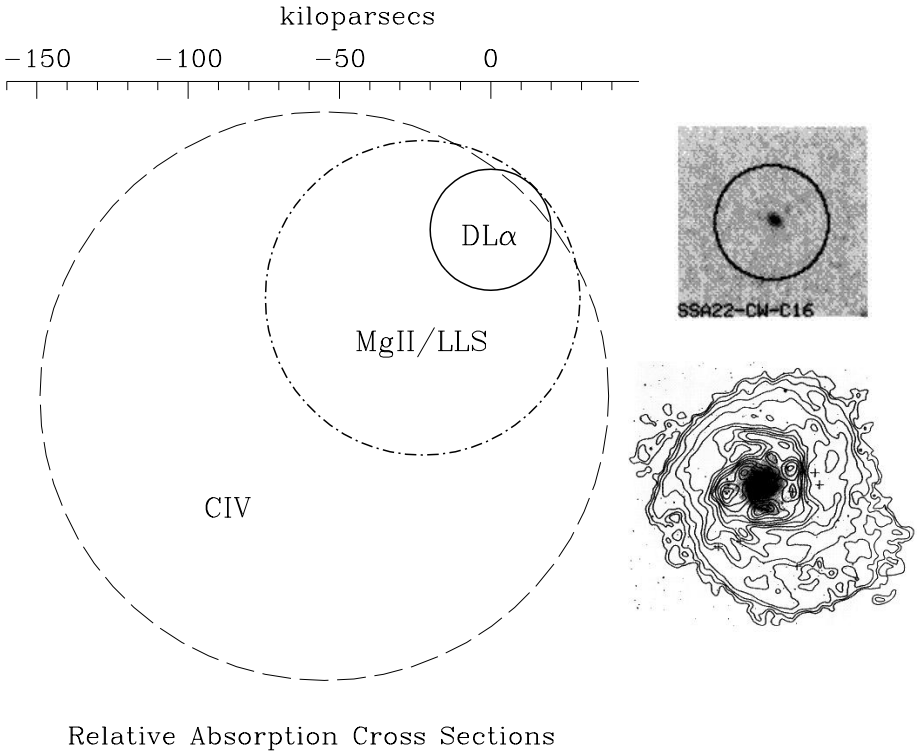

Figure 5. Comparison of quasar absorption-line cross sections for CIV, MgII-Lyman Limit, and damped Lyman$-\alpha$ lines with the physical size of the optical emission from a color-selected galaxy at $z \approx 3$ *top right* (Giavalisco et al 1996a) and the HI extent of a nearby, large $L \sim L_*$ galaxy M74=NGC628 *lower right* (Kamphuis & Briggs 1993). The absorption cross-sections are taken from Steidel 1993 and adapted to $H_o = 75$ km s^{-1}Mpc^{-1}. The $z \approx 3$ galaxy is centered in a $5''$ diameter circle that subtends 37.5 kpc ($\Omega_M = 0.2, \Omega_\Lambda = 0$). The Holmberg diameter of NGC628 is $\sim$36 kpc at a distance of 10 Mpc; the outermost contour is 1.3×10^{19}cm^{-2} and over half of the absorbing cross section is above 10^{20}cm^{-2}.

for different ions. Indeed, the the statistics show that the different species have different redshift dependencies over these ranges, so that the figure serves only as a rough illustration that the cross sections in CIV and MgII are substantially larger than the sizes of galaxy disks at $z = 0$, a conclusion that has led to the hypothesis of "metal-rich gaseous halos around galaxies." A variety of processes could fill halos with gas after metal enrichment by galactic stars; these include winds from star forming regions and tidal effects during merging and interactions with companion galaxies. The MgII gas arises in predominantly neutral gas clouds, although the column densities can be as low as $N_{HI}\sim10^{17}$cm^{-2}; this same column density is the critical level where gas clouds become optically thick to photons capable of ionizing hydrogen, so there is a direct association of MgII with the QSO absorption systems that are "optically thick at the Lyman limit," i.e., the systems known as either Lyman Limit or Lyman Continuum absorbers.

The statistics that give rise to the cross sections in Fig. 5 are based on strong

absorption line complexes of the sort expected along lines of sight through galaxies with metal rich halo gas. More recent studies using the high resolution spectrographs at Keck and VLT are sensitive to weaker equivalent width thresholds. These new studies have been effective at tracing the rise in metalicity of the intervening gas clouds in evolving galaxies with increasing age of the Universe (Pettini et al 2002, Prochaska et al 2003). In addition, they have discovered weak metal lines even in the Lα forest clouds (Lu 1991, Pettini et al 2003).

Figure 5 also compares the absorption cross sections with the observed sizes of the color-selected "Lyman break" galaxies at redshifts $z \sim 3$ and a large L^* spiral, M74, observed in the 21cm line nearby at $z \sim 0$. Although the large HI extent shown by M74 is not rare among nearby galaxies, such large cross sections are certainly in the minority, implying that cross sections of neutral gas were larger in the past. The Lyman break galaxies are somewhat less common that the comoving number density of L^* galaxies, implying that for every tiny, but highly luminous star forming system of the sort seen in the HST imaging, there must also be roughly double the gas-cloud cross-section drawn in the Figure, which must exist as low surface brightness or non-luminous material at these redshifts.

Absorption line observers also quantify the relative numbers of low and high column density absorbers. The distribution function $f(N_{HI})dN_{HI}$ (the "F-of-N" distribution) specifies the number of absorbers per unit redshift with N_{HI} in the column density range N_{HI} to $N_{HI} + dN_{HI}$. Over nearly ten orders of magnitude of column density, $f(N_{HI})$ can be approximated as $f(N_{HI}) = N_o N_{HI}^{-1.5}$, a single power-law which applies surprisingly well throughout the Lyman-α forest through to the DLA lines. When speaking of the relative frequency of occurrence of different column densities, it is convenient to use the number per logarithmic interval (say, per decade) and define an $F(N_{HI})d(\log_{10} N_{HI}) = f(N_{HI})dN_{HI}$. Then $F(N_{HI}) = N_o \ln(10) N^{-0.5}$ interceptions per decade, a shallower decline with column density than $f(N_{HI})$. The implication is that absorption lines with HI column density in the decade around 10^{17} are one-tenth as frequent as column densities in the decade centered on 10^{19}, for example.

A natural question to ask under these circumstances when the "$f(N)$" statistics indicate that low N_{HI} clouds are more common than high N_{HI} is: Which column densities contain more mass? The total neutral mass contained in the distribution comes from integrating $\int Nf(N)dN = \int NF(N)d(\ln N) = \int N^{0.5} d(\ln N)$, implying that the high mass end of the distribution dominates in the amount of *neutral* gas per logarithmic interval. The lower N_{HI} clouds are numerous, but when integrated up, they contain less neutral HI. However, since the low N_{HI} forest clouds are *highly ionized*, the HI that is seen in these clouds (with $N_{HI} < 10^{17} \mathrm{cm}^{-2}$) is just the tip of the iceberg of total mass contained in the clouds – the ionized hydrogen in the Lyman-α forest clouds accounts for many of the missing baryons of Fig.1. It is also clear that the expression for integral mass diverges at the large N limit, so that there must be some physical cutoff to the high column $f(N)$ distribution (Boissier et al 2003).

4.2 21cm line studies

The next generation of radio telescopes will be able to measure HI in galaxies to high redshifts (Taylor & Braun 1998, van Haarlem 1999), but our present telescopes are limited to doing absorption line studies that are similar to those done optically. The 21cm HI line is much weaker than the HI Lyman-α line: the optical depths at line center are in the ratio $\tau_{L\alpha}/\tau_{21cm} \approx 3{\times}10^8(T_s/100)$, explaining why only the highest column densities of cool hydrogen are detected in absorption at in the 21cm line. The dependence on spin temperature is a consequence of the correction for stimulated emission that arises because the upper level of the hyperfine splitting are always populated under normal astrophysical conditions (Spitzer 19XX). A further implication is that the gas temperature can be measured through a combination of the measurements of the two optical depths (one at UV/optical wavelengths and one at radio frequencies). When this remote sensing "thermometer" is applied to QSO absorption line systems as a function of redshift, a strong trend is observed that higher redshift systems become significantly warmer with increasing redshift and that this effect is strongly correlated with lower metalicity and the associated lower gas cooling rates (Kanekar & Chengalur 2003).

A virtue of 21cm absorption line studies against high redshift radio sources is that some background radio sources have very large physical extent, allowing them to backlight large areas of the foreground absorbing galaxy. Several such cases have been studied (Briggs et al 1989, Briggs et al 2001), and hundreds more will be accessible with future radio telescopes.

The principal question to be addressed is whether the gas-rich galaxies (such as the systems selected through DLA surveys) are large systems in orderly rotation like spiral galaxies or are aggregates of numerous smaller dwarfs systems with more random velocities that are in the process of merging, or are somewhere in between. Gas tracers like the 21cm line, which senses cold gas even in the absence of stars, has an important role to play in analyzing the physical sizes and dynamical masses of primitive systems, prior to them having established themselves as optically luminous galaxies.

Fig.6 illustrates how a disk galaxy leaves its imprint on the background radio source. When observed with a radio telescope of sufficient sensitivity and resolution, we expect to see the signs of rotation in the velocity field in the disk galaxy at $z_{abs} = 0.395$ that is absorbing against the background radio source at $z_{em} = 1.045$. The present resolution is only adequate to confirm that the HI optical depth is only significant against the western lobe of the source, which is consistent with the presence of an optically luminous galaxy close to this sight line.

5 Ionization, Reionization, and Re-reionization

Figure 1 summarizes the principal historical phases in the evolution of the neutral gas content of the Universe. Recombination at the time of the release of the CMB photons led to a period when the vast majority of the Universal baryons found themselves in neutral atoms. Once sources of ionization formed in the earliest astrophysical structures, the survival of neutral clouds has been a competition

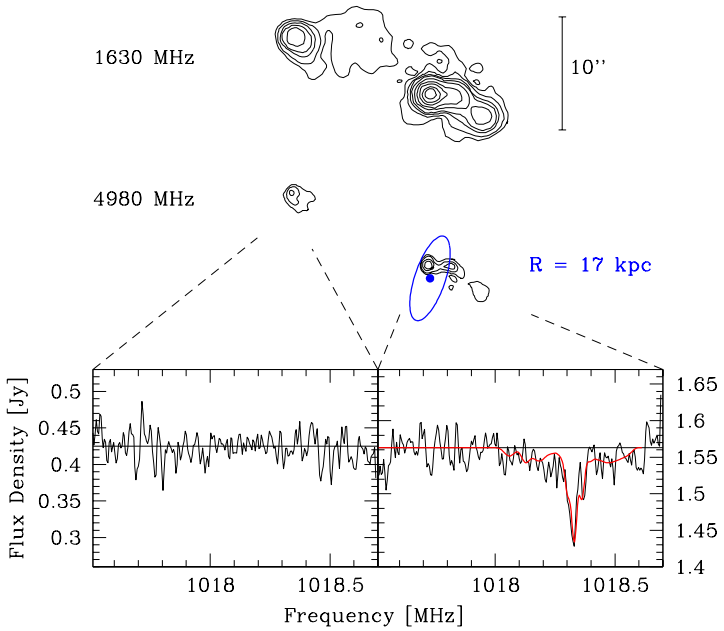

Figure 6. Radio 21cm HI absorption against the extended radio source PKS1229-021. The 21cm absorption occurs at $z = 0.395$, corresponding to 1018 MHz. As an interferometer, the WSRT has just enough resolution to decompose the absorption spectrum into the separate spectra for the two principal components of the radio emission (Briggs, Lane & de Bruyn 2004). The VLA contour maps shown here for the higher frequencies (Kronberg et al 1992) have better angular resolution but poor sensitivity to extended emission at 4980 MHz. The absorption, which only occurs against the righhand component, may have broad wings corresponding to absorption by a rotating system (the disk in the schematic representation), giving rise to opacity that is distributed across the face of the western component of the radio source. The oval is centered on the known location of an optically luminous galaxy in HST imaging (Le Brun et al 1999).

between ionization and recombination rates.

5.1 The ionization/recombination competition

Since ionization is such a common hazard to the existence of neutral atoms, it is natural to ask, "how rapidly can an ion recover through recombination, if it does chance to become ionized?" For hydrogen, the recombination rate R is easily computed (for instance Spitzer 197X), and the time t_{recomb} it takes for recombination to eliminate the electrons in a cloud of electron density n_e is

$$t_{recomb} = \frac{n_e}{R} = \frac{n_e}{n_e n_p \alpha_{recomb}} = \frac{1}{n_p \alpha_{recomb}} \approx \frac{T^{1/2}}{2{\times}10^{-11} n_p} \quad \text{sec} \tag{3}$$

where n_p is the proton density and α_{recomb} is the recombination coefficient. To get a feeling for the vulnerability of the bulk of the baryons that populate the intergalactic medium, the number density of baryons n_{baryon} forms an estimate of n_p; overdense regions will have relatively shorter recombination times. In an

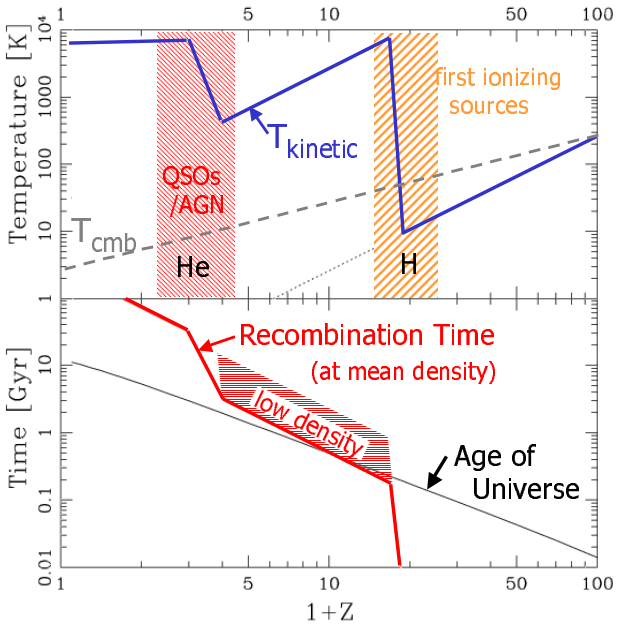

Figure 7. Recombination time in the intergalactic medium as a function of redshift z. *Upper Panel:* Kinetic temperature T_k and CMB temperature T_{CMB} vs. redshift. Episodes of heating through photoionization of hydrogen occur during the Epoch of Reionization and during the reionization of helium at a later time by the harder radiation from active galactic nuclei. *Lower Panel:* Recombination Time for an intergalactic medium of mean baryonic density, compared with the Age of the Universe as a function of redshift.

expanding Universe, $n_p \sim n_{baryon} \sim (1+z)^3$, so that

$$t_{recomb} \propto \frac{T^{1/2}}{(1+z)^3} \tag{4}$$

The recombination time of the IGM at mean density has a strong dependence on age of the Universe through the $(1+z)^3$, and a modest dependence on temperature T. Fig. 7 provides a rough illustration of how the IGM temperature varies with time and the net influence of the dependencies in Eqn. 4 on the ionization state of the Universe.

If the expansion of the Universe would allow a completely uniform expansion of the IGM without the growth of gravitationally-driven density instabilities, the gas kinetic temperature would decline in the adiabatic expansion with dependence $T_k \propto (1+z)^2$. At the same time, the CMB radiation temperature declines as $T_{CMB} \propto (1+z)^{-1}$, causing the two temperatures to decouple after $z \approx 100$, when electron scattering ceases to be effective. The IGM is reheated when photoionization spreads through the medium generating energetic photoelectrons that deposit their kinetic energy through scattering. Once the IGM is fully ionized, there is no effective means of adding energy to the gas, since the photons generated by the stars can now flow uninhibited through a transparent medium, and the IGM again cools

adiabatically due to Universal expansion.

A similar heating event can occur during the age around $z \sim 2$ when QSOs are most common. QSOs, as well as lesser AGN, radiate photons that are capabable of ionizing helium, and these harder photons generate photoelectrons throughout the IGM, providing a second round of localized heating.

The two heating events impact on the ability of the Universe to recombine. The lower panel of Fig. 7 compares the recombination time t_{recomb} of an IGM of mean density to the age of the Universe t_{age} as a function of redshift. If t_{recomb} is long compared to t_{age}, the IGM would never recover from its ionized state, even if the source of ionizing photons were turned off completely. The figure shows that there is period between the two heating events, when recombination can compete with ionization, depending on 1) the intensity of the ionizing flux and 2) the local density. Underdense regions would already be destined to stay forever ionized. Overdensities, especially those clouds confined in gravitational potential wells, may be able to recombine.

At low redshifts, the density of the mean IGM has become so dilute, that the IGM will remain ionized, even though the photoionizing background from AGN tails off.

The existence of atomic hydgrogen clouds at all at low redshift is due to their confinement to high density (greater than $\sim$0.1 cm^{-3}) where the recombination times are $< 10^5$yrs, and recombination can compete effectively to make self-shielding clouds.

5.2 EoR: The end of the Dark Age

The Epoch of Reionization that ends the Dark Age is now the subject of intense observational and theoretical interest. When and how do the first stars light up and begin the process of ionization and reheating? Several fine review articles summarize the current views (see for example, Barkana and Loeb 2001, Miralda-Escudé 2003). One of the findings of the Wilkinson Microwave Anisoptropy Probe (WMAP) has been a measurement of the optical depth to electron scattering between us and the so-called "surface of last scattering" at redshift around $z = 1089$. This optical depth in turn specifies a minimum redshift ($z_{reion} = 17 \pm 4$ according to Spergel et al 2003) when the bulk of the reionization must have taken place. This value for z_{reion} is at odds with measurements of the Gunn-Peterson effect that are consistent with the bulk of reionization occuring at $z_{gp} = 6.2$ (Gnedin 2001, Pentericci et al 2002). This conflict of the two measurements has led to a variety of models that invoke a "smouldering" or even double reionization (Gnedin & Shandarin 2002, Cen 2003). The idea as outlined in Section5.1 is that the IGM density is high enough at redshifts $z > 10$ that recombination is still effective. A continuing source of ionizing photons is required to maintain the ionization of the IGM. To continue to do this with stellar sources carries the implication of ongoing metal production, which runs the danger of generating more metals than are observing in the IGM.

The LOFAR (Low Frequency Array) and SKA (Square Kilometre Array) radio telescopes, whose design and construction are taking place over the next 15 years,

promise to allow astronomers to look into the EoR in the redshifted 21cm line at frequencies of 80 to 200 MHz, corresponding to the redshift range $z = 17$ to 6.2 discussed above. Unlike the WMAP result, which is an integral measurement of the electron content on a large angular scale, the 21cm observation will map the structure definted by the neutral clouds in three dimensions, resolving the neutral IGM both in angle on the sky and in depth through spectral resolution (Tozzi et al 2000, Furlanetto & Loeb 2002, Furlanetto et al 2003, Chen & Miralda-Escudé 2003). Thus, these instruments will not only clarify the timing of when the first stars form, but they will also monitor the growth of structure in the neutral component of the IGM through a period that promises to be complex and highly dependent on the astrophysics of material of primordial composition. Therefore, the star formation mechanisms at work will be unlike those we can study easily in the nearby star forming regions at $z \approx 0$.

References

1. Barkana, R., Loeb, A. 2001, ARA&A, 39, 19
2. Blitz, L. et al 1999, ApJ, 514, 818
3. Boissier, S., Peroux, C., Pettini, M. 2003, 338, 131
4. Braun, R. and Burton, W.B. 1999, A&A, 341, 437
5. Briggs, F.H. 1989, ApJ, 341, 650
6. Briggs, F.H. 1990, AJ, 100, 999
7. Briggs, F.H., de Bruyn, A.G., Vermeulen, R.C. 2001, A&A, 373, 113
8. Cen, R. 2003, ApJ, 591, 12
9. Chen, X., Miralda-Escudé, J. 2003, astro-ph/0303395
10. Fisher, J.R., & Tully, B. 1981, ApJ, 243, L32
11. Furlanetto, S., Loeb, A. 2002, ApJ, 579, 1
12. Furlanetto, S. et al 2003, astro-ph/0305065
13. Giavalisco, M., Steidel, C.C, Macchetto, F.D. 1996, ApJ, 470
14. Gnedin, N.Y. 2001, astro-ph/0110290
15. Gnedin, N.Y., Shandarin, S.F. 2002, MNRAS, 337, 1435
16. van Haarlem, M., ed. 1999, "Perspectives on Radio Astronomy: Science with Large Antenna Arrays," Proceedings of a conference held in Amsterdam in April 1999, (ISBN: 90-805434-1-1)
17. Haehnelt, M., Steinmetz, M., Rauch, M. 1998, ApJ, 495, 647
18. Kamphuis & Briggs 1993, A&A, 253, 335
19. Kanekar, N., Chengalur, J.N. 2003, A&A, 399, 857
20. Koribalksi, B. et al 2003, submitted
21. Kraan-Korteweg, R.C., et al 1999, A&AS, 135, 225
22. Kronberg, P.P., Perry, J.J., Zukowski, E.L.H. 1992, ApJ, 387, 528
23. Le Brun, V., et al 1997, A&A, 321, 733
24. Liszt, H. 2001, A&A, 371, 698
25. Lu, L. 1991, ApJ, 379, 99
26. Madgwick, D.S. et al 2002, MNRAS, 333, 133
27. Miralda-Escudé, J. 2003, Sci, 300, 1904
28. Olive, K.A., Steigman, G., Walker, T.P. 2000, PhR, 333, 389

29. Oosterloo, T., et al, 2003, IAUS, 217, 108
30. Pentericci, L., et al 2002, AJ, 123, 2151
31. Penton, S.V., Shull, J.M., Stocke, J.T. 2000, ApJ, 544, 150
32. Pettini, M., et al 2002, A&A, 391,21
33. Pettini, M., et al 2003, ApJ, 594, 695
34. Prochaska, J.X., Wolfe, A.M. 1997, ApJ, 487, 73
35. Prochaska, J.X., Howk, J.C., Wolfe, A.M. 2003, Nature, 423, 57
36. Prochaska, J.A., et al 2003, ApJ, 595, L9
37. Roberts, M.S., Haynes, M.P. 1994, ARA&A, 32, 115
38. Rosenberg, J.L. & Schneider, S.E. 2000, ApJS, 130, 177
39. Schechter, P. 1976, ApJ, 203, 297
40. Shull, J.M. 2003, in The IGM/Galaxy Connection: The Distribution of Baryons at z=0, ASSL Conference Proceedings Vol. 281, J.L. Rosenberg & M.E. Putman, eds, Kluwer Academic Publ, p.1
41. Spergel, D.N. et al 2003, ApJS, 148, 175
42. Spitzak, J. & Schneider, s.E. 1998, ApJS, 119, 159
43. Spitzer book (for recomb rate)
44. Steidel, C.C. 1993, in The Environment and Evolution of Galaxies, eds. J. Shull & H.A. Thronson, Kluwer Academic Publ, p. 263
45. Taylor, A.R., Braun, R. 1998, Science with the SKA, see http://www.skatelescope.org/ska_science.shtml
46. Tozzi, P., et al 2000, ApJ, 528, 597
47. Wolfe, A.M., et al 1986, ApJS, 61, 249
48. Wolfire, M.G., et al 2003, ApJ, 587, 278
49. Zwaan, M.A., et al 1997, ApJ, 490, 173
50. Zwaan, M.A., & Briggs, F.H. 2000, ApJ, 530L, 61
51. Zwaan, M.A. 2001, MNRAS, 325, 1142
52. Zwaan, M.A., et al, 2003, AJ, 125, 2842